Dynamics of charge transport in planar devices

F. Beunis,[1,*] F. Strubbe,[1] M. Marescaux,[1] J. Beeckman,[1] K. Neyts,[1] and A. R. M. Verschueren[2]
[1]*ELIS department, Ghent University, Sint Pietersnieuwstraat 41, B-9000 Ghent, Belgium*
[2]*Philips Research Laboratories, High Tech Campus 34, 5656 AE Eindhoven, The Netherlands*
(Received 23 January 2008; revised manuscript received 26 May 2008; published 17 July 2008)

The Poisson-Nernst-Planck equations describe the dynamics of charge transport in an electric field. Although they are relevant in many applications, a general solution is not known and several aspects are not well understood. In many situations nonlinear effects arise for which no analytical description is available. In this work, we investigate charge transport in a planar device on application of a voltage step. We derive analytical expressions for the dynamical behavior in four extreme cases. In the "geometry limited" regime, applicable at high voltages and low charge contents, we neglect diffusion and the electric field induced by the charges. This leads to a uniform movement of all charges until the bulk is completely depleted. In the "space charge limited" regime, for high voltages and high charge contents, diffusion is still neglected but the electric field is almost completely screened over transient space charge layers. Eventually, however, the bulk becomes depleted of charges and the field becomes homogeneous again. This regime is solved under the assumption of a homogeneous current density, and is characterized by a typical $t^{-3/4}$ behavior. In the "diffusion limited" regime, valid for low voltages and low charge contents, diffusion is the dominant transport mechanism and prevents the charges from separating. This results in only very small deviations from a homogeneous charge distribution throughout the device. In the "double layer limited" regime, for low voltages and high charge contents, the combination of dominant diffusion and screening of the electric field results in large variations occurring only in thin double layers near the electrodes. Numerical simulations confirm the validity of the derived analytical expressions for each of the four regimes, and allow us to investigate the parameter values for which they are applicable. We present transient current measurements on a nonpolar liquid with surfactant and compare them with the external current predicted by the theoretical description. The agreement of the analytical expressions with the experiments allows us to obtain values for a number of properties of the charges in the liquid, which are consistent with results in other works. The confirmation by simulations and measurements of the derived theoretical expressions gives confidence about their usefulness to understand various aspects of the Poisson-Nernst-Planck equations and the effects they represent in the dynamics of charge transport.

DOI: 10.1103/PhysRevE.78.011502 PACS number(s): 82.45.Gj, 66.10.−x, 47.57.jd

I. INTRODUCTION

The movement of charges in a viscous medium under the influence of an electric field in a plan-parallel device is a very general problem [1,2]. It lies at the basis of the understanding of electrolytes [3–5], colloidal systems [6,7], semiconductors [8–11], plasmas [12,13] and many other applications. The Poisson-Nernst-Planck equations model the effects of thermal diffusion and drift in the electric field on the charges and the induced change in the electric field by the charges. In most applications other equations have to be added to model mechanisms such as chemical reactions in the bulk [14,15] or at the electrodes [16] or to include sterical effects [17,18], but the basic problem is always the same. However, despite the importance of the Poisson-Nernst-Planck equations, no general solution is known.

The behavior of charges in a planar structure can be radically different, depending on the properties of the device and on the driving conditions [1,19]. In the case of thick devices with a high charge content, driven at relatively small voltages, which is the relevant situation in many applications, the Poisson-Nernst-Planck equations can be linearized and solved [1,19]. However, for larger voltages, in thin devices or for lower charge concentrations, nonlinear effects [1,19,20] make the solution much more difficult. These situations become increasingly important with the ongoing miniaturization and with the growing use of non-polar media, such as in liquid crystal displays [21,22] and electrophoretic ink [23,24].

These nonlinear effects are usually treated as higher order deviations from the linear case [1]. However, we take a different approach and investigate four extreme cases (one of them being of course the linear case). These regimes provide an understanding of the dominant effects in cases which are not well understood today, and provide a different perspective to investigate the Poisson-Nernst-Planck equations.

In this work we investigate the dynamical behavior on application of a voltage on a plan-parallel device which has been short-circuited for a long time. We derive approximate analytical expressions for the charge distribution and electric field in function of time and position, for each of the four regimes. These theoretical expressions are valid for a broad range of applications. The analytical descriptions are then compared with numerical simulations and with current measurements on a mixture of dodecane and a surfactant [14,25]. This mixture can, depending on the conditions, exhibit the behavior of each of the four regimes, and therefore acts as a model system for the theoretical problem investigated in this work. The analytical expressions for the current provide a way to determine several properties of the mixture, such as

*Filip.Beunis@ELIS.UGent.be

the concentration, mobility, and valency of the charges. A similar approach has been followed in another work [26] to derive analytical expressions for the steady state distribution of charges in an electric field, which are confirmed by measurements.

II. THEORETICAL ANALYSIS

We approximate the plan-parallel device with a one-dimensional structure, in which all quantities are only dependent on the spatial coordinate x and on the time t. This structure is bound by two electrodes separated by a distance d. The reference position $x=0$ is chosen in the middle of the structure, so the left electrode is at position $x=-d/2$ and the right electrode at position $x=d/2$. Between the two electrodes, we consider a symmetric electrolyte, approximated by a dielectric medium in which positive and negative charges are present, which are identical except for their polarity. The dielectric permittivity of this medium is $\epsilon\epsilon_0$, with ϵ_0 the dielectric permittivity of vacuum and ϵ the relative dielectric constant of the medium. The charges carry a charge $\pm q$ and their distribution in the medium is described by the concentrations $n_+(x,t)$ (m^{-3}) and $n_-(x,t)$ (m^{-3}) for positive and negative charges, respectively. We will also use the charge concentration $\rho(x,t)$ $(\mathrm{C\ m}^{-3})$ and the total concentration $m(x,t)$ (m^{-3}), related to n_+ and n_- by $\rho=q(n_+-n_-)$ and $m=n_++n_-$.

For $t<0$, the electrodes are at the same potential, and all charges are homogeneously distributed. At the reference time $(t=0)$, a voltage V_A is applied over the electrodes, so that the left electrode is at potential $V_A/2$ and the right electrode is at potential $-V_A/2$. The electric field strength $E(x,t)$, which we measure in the positive x direction, is related to this voltage through

$$\int_{-d/2}^{d/2} E dx = V_A, \tag{1}$$

and to the distribution of charges through Gauss's equation (which is equivalent to Poisson's equation):

$$\epsilon\epsilon_0 \frac{\partial E}{\partial x} = \rho. \tag{2}$$

The movement of the charges is the result of drift in the electric field and thermal diffusion. It can be described by the Nernst-Planck equation [1]

$$\Psi_\pm = \pm \mu n_\pm E - D\frac{\partial n_\pm}{\partial x}. \tag{3}$$

$\Psi_+(x,t)$ $(\mathrm{m}^{-2}\ \mathrm{s}^{-1})$ and $\Psi_-(x,t)$ $(\mathrm{m}^{-2}\ \mathrm{s}^{-1})$ are the fluxes of positive and negative charges in the positive x direction. The mobility μ and the diffusion constant D are assumed to be the same for positive and negative charges and are related by Einstein's formula $D/\mu=V_T$. The thermal voltage V_T is defined as kT/q, in which k is Boltzmann's constant and T is the absolute temperature of the device. We assume that no charges can appear or disappear in the bulk, so the following continuity equation holds

$$\frac{\partial n_\pm}{\partial t} = -\frac{\partial \Psi_\pm}{\partial x}. \tag{4}$$

We assume perfectly blocking electrodes, so at the boundaries of the structure no charges can appear or disappear, and the fluxes there have to be zero, so $\Psi_\pm(-d/2,t)=0$ and $\Psi_\pm(d/2,t)=0$. As a result of these boundary conditions and Eqs. (3) and (4), the average concentrations of positive and negative charges have to be constant in time. We assume global neutrality, so both average concentrations have to be equal, and this value is defined as $\bar{n}=\frac{1}{d}\int_{-d/2}^{d/2} n_\pm dx$. Equivalently, the total charge in the device per unit electrode surface $Q_{\mathrm{tot}}=q\int_{-d/2}^{d/2} n_\pm dx = q\bar{n}d$ is constant in time.

The charge (per unit of electrode surface) $Q_{\mathrm{el}}(t)$ on the left electrode (and $-Q_{\mathrm{el}}$ on the right electrode) consists of electrons or holes, so it is of a different nature than the charges in the liquid. It is the sum of two contributions: a capacitive charge Q_{cap} as a result of the applied voltage, and an induced charge $Q_{\mathrm{ind}}(t)$ as a result of the charge between the electrodes: $Q_{\mathrm{el}}=Q_{\mathrm{cap}}+Q_{\mathrm{ind}}$. The capacitive charge can be expressed as $Q_{\mathrm{cap}}=\epsilon\epsilon_0 V_A/d$ and the induced charge can be calculated using Ramo's theorem [27], which states that (with the assumptions made in this work) the induced charge is proportional with the first geometrical momentum of the charge distribution: $Q_{\mathrm{ind}}=\frac{1}{d}\int_{-d/2}^{d/2}\rho x dx$. The external current (per unit of electrode surface) $I(t)$, flowing toward the left electrode and away from the right electrode, is then $I=dQ_{\mathrm{el}}/dt=Q_{\mathrm{cap}}\delta(t)+dQ_{\mathrm{ind}}/dt$. The Dirac impulse is a result of the voltage step and the fact that we consider the electrodes to be perfect conductors, and will be omitted in the rest of this work. The external current can then be calculated, using Eqs. (1) and (2) and the fact that E is symmetric around $x=0$, as

$$I = \epsilon\epsilon_0 \frac{dE(\pm\frac{d}{2},t)}{dt}, \tag{5}$$

or, using Eq. (4), as

$$I = \frac{1}{d}\int_{-d/2}^{d/2} J dx, \tag{6}$$

in which $J(x,t)$ is the current density inside the structure $J=q(\Psi_+-\Psi_-)$.

At $t=0$ the concentrations $n_\pm$ are homogeneous, so the second term in Eq. (3), which represents diffusion, is zero. Since the concentrations are also equal, the charge concentration ρ is zero and, because of Eq. (2), the electric field E is homogeneous and, because of Eq. (1), the field is equal to V_A/d. Using Eqs. (3) and (6) we find therefore the following expression for the initial current I_0:

$$I_0 = \frac{2q\bar{n}\mu V_A}{d}. \tag{7}$$

After $t=0$, The current will decrease because of a combination of three different reasons. The first reason is a result of the geometry of the structure: when charges reach the electrodes at $x=\pm d/2$, they cannot move any further and stop contributing to the current. The second reason is diffusion,

which, as can be seen in Eq. (3), tends to displace the charges toward the original homogeneous distribution, thereby preventing them to separate completely. The third reason is (partial or almost complete) screening of the electric field: when charges become separated, the electric field in the bulk will decrease as a result of Eqs. (1) and (2), and this slows down the separation of charges by drift. Each of these reasons can be more or less important, depending on different parameters. In Sec. III of this work we discuss in more detail the conditions which determine the relative importance of the different effects, but already now it can be understood intuitively that the effect of diffusion is lower for higher voltages V_A (compared to the thermal voltage V_T) and the effect of screening is higher for a higher total charge Q_{tot} (compared to the capacitive charge Q_{cap}). The effect of the geometry is always present.

The Poisson-Nernst-Planck equations can be written in the following dimensionless form

$$\tilde{\Psi}_{\pm} = \pm \tilde{n}_{\pm}\tilde{E} - \frac{1}{\tilde{V}_A}\frac{\partial \tilde{n}_{\pm}}{\partial \tilde{x}}, \tag{8}$$

$$\frac{\partial \tilde{\Psi}_{\pm}}{\partial \tilde{x}} = -\frac{1}{\tilde{V}_A}\frac{\partial \tilde{n}_{\pm}}{\partial \tilde{t}}, \tag{9}$$

$$\frac{\partial \tilde{E}}{\partial \tilde{x}} = \frac{\tilde{Q}_{\mathrm{tot}}}{2\tilde{V}_A}(\tilde{n}_+ - \tilde{n}_-), \tag{10}$$

$$\int_{-1/2}^{1/2} \tilde{E}\, d\tilde{x} = 1, \tag{11}$$

in which the dimensionless coordinates are defined as $\tilde{x} = x/d$ and $\tilde{t} = Dt/d^2$, and the dimensionless variables as $\tilde{n}_{\pm} = n_{\pm}/\bar{n}$, $\tilde{E} = Ed/V_A$, and $\tilde{\Psi}_{\pm} = 2q\Psi_{\pm}/I_0$. Equations (8)–(11) are only dependent on two dimensionless parameters

$$\tilde{V}_A = \frac{V_A}{V_T}, \tag{12}$$

$$\tilde{Q}_{\mathrm{tot}} = Q_{\mathrm{tot}} \Big/ \left(\frac{\epsilon\epsilon_0}{2d} V_T\right). \tag{13}$$

These two parameters are equivalent to the two dimensionless parameters v and ϵ used in Ref. [1], and are related to them by $\tilde{Q}_{\mathrm{tot}} = 1/\epsilon^2$ and $\tilde{V}_A = 2v$. It is possible to identify each possible situation with a point in the $(\tilde{V}_A, \tilde{Q}_{\mathrm{tot}})$ parameter plane. In this work, we will focus on values for $\tilde{V}_A$ between 0.1 and 1000 and values for $\tilde{Q}_{\mathrm{tot}}$ between 0.1 and 10^6. We will also use the following derived dimensionless quantities: $\tilde{\rho} = \rho/q\bar{n}$, $\tilde{m} = m/\bar{n}$, $\tilde{J} = J/I_0$, and $\tilde{I} = I/I_0$.

In the following paragraphs, we will discuss four limiting cases. In the "geometry limited" regime, the effects of diffusion and screening are completely neglected. In the "space charge limited" regime, diffusion is still neglected, but the charge content is so high that the electric field in the bulk is almost completely screened by transient space charge regions, which are formed as positive and negative charges become separated. In the "diffusion limited" regime, the voltage is so low that diffusion is dominant, but the total charge is also low enough so that the electric field remains homogeneous. Finally, in the "double layer limited" regime, the interplay between diffusion and screening in the limit of a very low voltage and a very high charge content results in the formation of diffuse double layers which almost completely screen the electric field in the bulk.

A. Regimes without diffusion

In the limiting case when drift is the dominant transport mechanism, we neglect the diffusion term in Eq. (3):

$$\Psi_{\pm} = \pm \mu n_{\pm} E. \tag{14}$$

The combination of Eq. (14) and the blocking electrode boundary conditions has some important consequences. A first consequence is that a positive surface charge builds up near the negative electrode and a negative surface charge builds up near the positive electrode. These surface charges have no effect on the electric field in the device since they are infinitesimally close to the electrodes and induce an exactly opposite image charge. A second consequence of neglecting diffusion is that, adjacent to the electrodes, space charge regions with thickness $\lambda_{\mathrm{SC}}(t)$ occur where charges of one polarity are completely absent, resulting in an unbalanced space charge of the other polarity.

We assume the boundaries of these space charge layers to be discontinuities in the concentrations of positive and negative charges. We will show that this assumption does not affect the limiting dynamics of the solution. However, even in the limit of very high voltages, the diffusion term in Eq. (8) will not be zero at these discontinuities. This will result in a smoothing of the sharp boundaries, which will be obvious in the numerical simulation results, but which is not described in the analytical treatment.

The dynamics of the space charge regions can be divided into two phases. In the first phase, the positive and negative space charge regions grow because of the movement of charges with the opposite polarity in the bulk between the space charge regions. During this separation phase, the concentrations n_+ and n_- in the bulk are equal to their initial value $\bar{n}$, resulting in a homogeneous electric field $E_{\mathrm{bulk}}(t)$. The charge distribution and the electric field in the whole device during the separation phase can therefore be described by

$$\begin{aligned} n_{\pm} &= 0 \quad \text{for} \quad -d/2 < \pm x < -(d/2 - \lambda_{\mathrm{SC}}), \\ n_{\pm} &= \bar{n} \quad \text{for} \quad -(d/2 - \lambda_{\mathrm{SC}}) < \pm x < (d/2 - \lambda_{\mathrm{SC}}), \\ n_{\pm} &= n_{\mathrm{SC}}(\pm x, t) \quad \text{for} \quad (d/2 - \lambda_{\mathrm{SC}}) < \pm x < d/2, \end{aligned} \tag{15}$$

and

$$\begin{aligned} E &= E_{\mathrm{SC}}(-x, t) \quad \text{for} \quad -d/2 < x < -(d/2 - \lambda_{\mathrm{SC}}), \\ E &= E_{\mathrm{bulk}}(t) \quad \text{for} \quad -(d/2 - \lambda_{\mathrm{SC}}) < x < (d/2 - \lambda_{\mathrm{SC}}), \end{aligned}$$

$$E = E_{SC}(x,t) \quad \text{for } (d/2 - \lambda_{SC}) < x < d/2, \tag{16}$$

in which $n_{SC}(x,t)$ and $E_{SC}(x,t)$ are functions which are equal to the concentration of positive charges and to the electric field in the space charge layer closest to the negative electrode. Since only one polarity is present in this region, Eq. (2) results in

$$n_{SC} = \frac{\epsilon\epsilon_0}{q}\frac{\partial E_{SC}}{\partial x}. \tag{17}$$

The speed at which the space charge regions grow is equal to the speed of the charges in the bulk

$$\frac{d\lambda_{SC}}{dt} = \mu E_{bulk}. \tag{18}$$

The second phase starts when the space charge layers occupy the whole device ($2\lambda_{SC}=d$) and positive and negative charges are completely separated. After this separation time τ_{sep}, the space charge regions shrink because of the movement of the charges inside the regions. In the bulk, n_+ and n_- are now both zero, so E_{bulk} is still homogeneous. Therefore, during this depletion phase, we have

$$n_\pm = 0 \quad \text{for } -d/2 < \pm x < -(d/2 - \lambda_{SC}),$$

$$n_\pm = 0 \quad \text{for } -(d/2 - \lambda_{SC}) < \pm x < (d/2 - \lambda_{SC}),$$

$$n_\pm = n_{SC}(\pm x,t) \quad \text{for } (d/2 - \lambda_{SC}) < \pm x < d/2. \tag{19}$$

The electric field is still described by Eq. (16). Because of continuity of the electric field, during the depletion phase the borders of the space charge layers move according to

$$\frac{d\lambda_{SC}}{dt} = -\mu E_{bulk}. \tag{20}$$

The depletion phase ends when the bulk is completely depleted of charges, at the depletion time τ_{dep}, and the steady state situation is reached. Since all charges are at the electrodes and compensated by an image charge on the electrodes, the induced charge Q_{ind} in steady state is equal to the total charge Q_{tot} in the device. We find then

$$\int_0^\infty I dt = Q_{tot}. \tag{21}$$

Depending on the total charge Q_{tot} in the device, the charge in the space charge regions will screen the electric field in the bulk partially or completely during the transient. In the following paragraphs, we will discuss the two limiting cases of an undisturbed field (the geometry limited regime) and of an almost completely screened field (the space charge limited regime).

1. Geometry limited regime

In the limiting case in which the electric field is not screened at all [28], Eqs. (1) and (2) can be replaced by $E = V_A/d$. The time dependency of the thickness of the space charge regions follows then from Eqs. (18) and (20):

$$\lambda_{SC} = \mu\frac{V_A}{d}t \quad \text{for } 0 \le t \le \tau_{sep} = \tau_{tr}/2 \text{ (separation phase)},$$

$$\lambda_{SC} = d - \mu\frac{V_A}{d}t \quad \text{for } \tau_{sep} \le t \le \tau_{dep} = \tau_{tr} \text{ (depletion phase)},$$

$$\lambda_{SC} = 0 \quad \text{for } \tau_{dep} \le t \text{ (steady state)} \tag{22}$$

in which the transit time τ_{tr} is the time that a charge needs to cross the whole thickness of the device when the field is not screened: $\tau_{tr} = d^2/\mu V_A$. Since the electric field is homogeneous, all charges move with the same speed, so the concentrations during the separation phase ($0 \le t \le \tau_{sep}$) are described by $n_{SC} = \bar{n}$. Using Eqs. (6) and (14), we find that the external current decreases linearly over time during both the separation and the depletion phase

$$I = I_0\left(1 - \frac{t}{\tau_{tr}}\right), \tag{23}$$

until steady state is reached at $t = \tau_{tr}$, after which the current remains zero.

The system of (dimensionless) Eqs. (8)–(11) has been solved numerically using a forward Euler algorithm, for different situations. In Fig. 1, the analytical formulas are compared with these numerical results for the case with $\tilde{Q}_{tot} = 0.1$ and $\tilde{V}_A = 1000$. This situation is representative for the geometry limited regime, as will be demonstrated in Sec. III. Figure 1 shows that the electric field is indeed homogeneous and constant over time. Because of this, the charges move at a homogeneous speed, and variations of the concentrations and current densities only occur at the borders between the bulk layer and the space charge layers. In the analytical formulas, these positions and the separation and depletion times are sharply defined, because of neglecting diffusion. In the simulation, with diffusion, the variations occur over broader intervals. However, it can be seen that this has no significant influence on the dynamics of the charge transport.

The surface charge Q_s can easily be calculated by taking the difference between the total charge and the integral of Eqs. (15) and (19): $Q_s = q\bar{n}\mu V_A t/d$. Now we introduce diffusion to find a more accurate description of the distribution of charges near the electrodes. The surface charge will then be spread out over a thin "double layer." We assume that the charge that was modeled as a surface charge, has in fact the same distribution as in steady state [26], so

$$n_{DL} = \frac{Q_s}{qd}\frac{V_A}{V_T}e^{V_A/V_T(1/2 - x/d)}, \tag{24}$$

in which $n_{DL}(x,t)$ is the extra concentration close to the negative electrode. Figure 2 shows that these expressions agree with the simulation results.

2. Space charge limited regime

When the charge content is sufficiently large, the charge in the space charge regions has an important screening effect on the electric field in the bulk. Therefore, the electric field

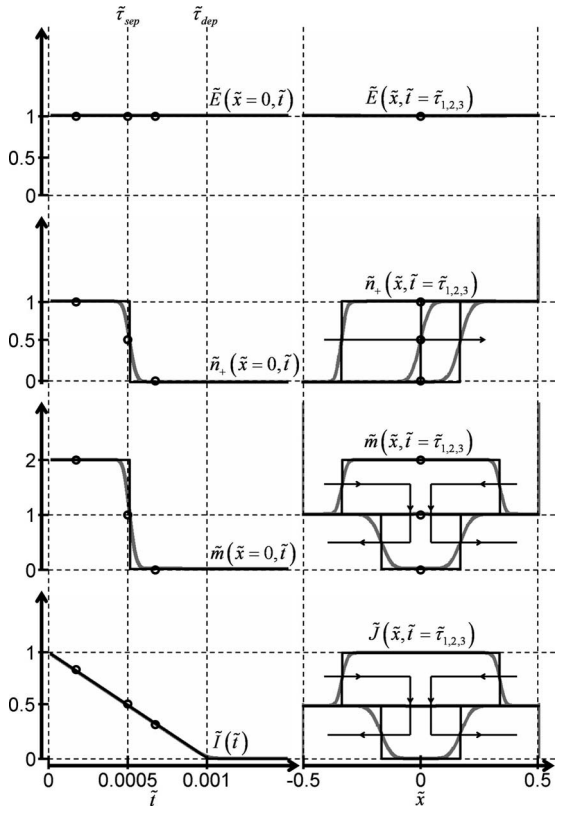

FIG. 1. Comparison between theory (black curves) and simulation (gray curves) for $\tilde{Q}_{\mathrm{tot}}=0.1$ and $\tilde{V}_A=1000$ (representative for the geometry limited regime). Where the gray curves are not visible, they are coinciding with the black curves. On the left, the electric field, the concentration of positive charges and the total concentration in the middle of the device, as well as the external current, are shown in function of time. On the right, the electric field, the concentration of positive charges, the total concentration and the current density are shown in function of place at times $\tilde{\tau}_1=0.000\,33$, $\tilde{\tau}_2=0.0005$, and $\tilde{\tau}_3=0.000\,67$. The dots on the left indicate these three times, the dots on the right indicate the position from the corresponding curves on the left.

in the bulk will be lower than the electric field in the space charge regions. During the separation phase, charges which move from the bulk region to a space charge region will accelerate in the inhomogeneous field, leading to an inhomogeneous concentration in the space charge regions. In Ref. [20], it was shown that in this situation, when drift is dominant and the field in the bulk region is almost completely screened, the electric current density J is approximately homogeneous over the whole device. In the section discussing the double layer limited regime we will see that this is also true when diffusion is present, making the homogeneity of the current density a typical characteristic if screening is a limiting mechanism. This can be understood by combining Eqs. (2) and (4) to obtain $\frac{\partial}{\partial x}(J+\epsilon\epsilon_0\frac{\partial}{\partial t}E)=0$. When the electric field is almost completely screened it cannot decrease much more. The high charge content, however, still results in a high current density. Therefore, the second term in this equation can be neglected compared to the first term, resulting in a homogeneous current density.

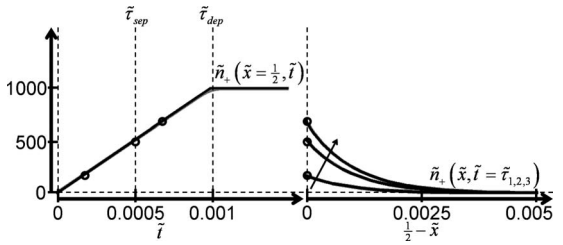

FIG. 2. Comparison between theory (black curves) and simulation (gray curves) for $\tilde{Q}_{\mathrm{tot}}=0.1$ and $\tilde{V}_A=1000$ (representative for the geometry limited regime). Where the gray curves are not visible, they are coinciding with the black curves. On the left, the concentration of positive charges at the electrode is shown in function of time. On the right, the concentration of positive charges in the double layer is shown in function of place at times $\tilde{\tau}_1=0.000\,33$, $\tilde{\tau}_2=0.0005$, and $\tilde{\tau}_3=0.000\,67$. The dots on the left indicate these three times, the dots on the right indicate the position from the corresponding curve on the left.

Using Eqs. (2) and (14), the equality of the current densities in the bulk and in the space charge regions leads to

$$\frac{\mu}{2}\frac{\partial}{\partial x}(E_{\mathrm{SC}}^2)=\frac{2\mu q\bar{n}}{\epsilon\epsilon_0}E_{\mathrm{bulk}}. \tag{25}$$

Using the continuity of the electric field at the boundary between the space charge regions and the bulk, the solution of this differential equation is

$$E_{\mathrm{SC}}=\sqrt{E_{\mathrm{bulk}}^2+\frac{4q\bar{n}}{\epsilon\epsilon_0}\left(x+\lambda_{\mathrm{SC}}-\frac{d}{2}\right)}E_{\mathrm{bulk}}. \tag{26}$$

We define the field in the space charge region near the right interface as $E_{\mathrm{int}}(t)=E_{\mathrm{SC}}(d/2,t)$, so

$$\frac{E_{\mathrm{int}}^2-E_{\mathrm{bulk}}^2}{E_{\mathrm{bulk}}}=\frac{4q\bar{n}}{\epsilon\epsilon_0}\lambda_{\mathrm{SC}}. \tag{27}$$

Note that E_{int} is not the same as the field at the electrode, used in Eq. (5), because there is a positive surface charge between the space charge region and the negative electrode.

We assume now that the voltage drop over the bulk region can be neglected compared to the voltage drop over the space charge regions. Using Eqs. (26) and (27), the integration of Eq. (1) results in

$$V_A=\frac{\epsilon\epsilon_0}{3q\bar{n}}\frac{E_{\mathrm{int}}^3-E_{\mathrm{bulk}}^3}{E_{\mathrm{bulk}}}. \tag{28}$$

Using Eqs. (27) and (28), in which we assume $E_{\mathrm{int}}\gg E_{\mathrm{bulk}}$, and Eq. (18), we find the following differential equation for λ_{SC}: $\frac{d}{dt}(\lambda_{\mathrm{SC}}^4)=\frac{9}{16}\mu\epsilon\epsilon_0V_A^2q^{-1}\bar{n}^{-1}$. With $\lambda_{\mathrm{SC}}(0)=0$ as initial condition, the solution of this differential equation is

$$\lambda_{\mathrm{SC}}=\frac{d}{2}\left(\frac{t}{\tau_{\mathrm{sep}}}\right)^{1/4}, \tag{29}$$

in which the separation time is given by

$$\tau_{\mathrm{sep}} = \frac{1}{8\gamma}\tau_{\mathrm{tr}}, \tag{30}$$

with the dimensionless factor γ defined as

$$\gamma = \frac{9}{8}\frac{Q_{\mathrm{cap}}}{Q_{\mathrm{tot}}}. \tag{31}$$

Using the fact that the electric current density is homogeneous over the whole device, the external current during the separation phase can be calculated as

$$I = \gamma I_0 \left(\frac{t}{\tau_{\mathrm{sep}}}\right)^{-3/4}. \tag{32}$$

At τ_{sep}, the space charge regions occupy the whole device, and cannot be supplied with charges from the bulk region anymore. During the depletion phase, the remaining charge in the space charge regions moves to the electrodes, λ_{SC} decreases to zero, the current drops to zero and the electric field becomes homogeneous. This happens fast compared to the decrease of the current during the separation phase, because the electric field in the space charge regions during the depletion phase is large compared to the electric field in the bulk during the separation phase. Therefore, we neglect the duration $\tau_{\mathrm{dep}}-\tau_{\mathrm{sep}}$ of the depletion phase compared to the duration of the separation phase τ_{sep}, so we assume $\tau_{\mathrm{dep}} \approx \tau_{\mathrm{sep}}$. With this assumption we find that, integrating the current as in Eqs. (32) and (21) holds: $\int_0^{\infty} I dt = \int_0^{\tau_{\mathrm{dep}}} I dt = \int_0^{\tau_{\mathrm{sep}}} I dt = Q_{\mathrm{tot}}$.

At $t=0$, the expression for the current in Eq. (32) becomes infinitely high. The reason for this is that the assumption that the field is screened does not hold at very short times (at $t=0$, the field is homogeneous and the current should be I_0). Therefore, we define the screening time τ_{scr} as the time at which the current in Eq. (32) becomes equal to I_0, after which we assume that the screening assumption is justified. τ_{scr} can be calculated as

$$\tau_{\mathrm{scr}} = \frac{\gamma^{1/3}}{8}\tau_{\mathrm{tr}}. \tag{33}$$

Before this screening time we assume that the current remains approximately equal to I_0. However, with this assumption the integral of the current is not equal to Q_{tot} anymore. Therefore, we renormalize the current during the separation phase by introducing γ', defined by the condition $\tau_{\mathrm{scr}} I_0 + \frac{\gamma'}{\gamma}\int_{\tau_{\mathrm{scr}}}^{\tau_{\mathrm{sep}}} I dt = Q_{\mathrm{tot}}$. The new factor γ' can then be calculated to be

$$\gamma' = \frac{1-\frac{1}{4}\gamma^{1/3}}{1-\gamma^{1/3}}\gamma. \tag{34}$$

The current is then

$$I = I_0 \quad \text{for} \quad 0 \le t \le \tau_{\mathrm{scr}} \quad \text{(screening phase)},$$

$$I = \gamma' I_0 \left(\frac{t}{\tau_{\mathrm{sep}}}\right)^{-3/4} \quad \text{for} \quad \tau_{\mathrm{scr}} \le t \le \tau_{\mathrm{sep}} \quad \text{(separation phase)},$$

$$I = \gamma' I_0 \quad \text{for} \quad \tau_{\mathrm{sep}} = t = \tau_{\mathrm{dep}} \quad \text{(depletion phase)},$$

$$I = 0 \quad \text{for} \quad \tau_{\mathrm{dep}} \le t \quad \text{(steady state)}. \tag{35}$$

In Eq. (25), both sides are equal to the current density J. Since J is homogeneous, they are also equal to the external current I, which allows us to calculate E_{bulk}:

$$E_{\mathrm{bulk}} = \gamma' \frac{V_A}{d}\left(\frac{t}{\tau_{\mathrm{sep}}}\right)^{-3/4}. \tag{36}$$

The first order approximation of λ_{SC} in Eq. (29) can be improved by substituting Eq. (18) in Eq. (36). Using the condition $\lambda_{\mathrm{SC}}(\tau_{\mathrm{sep}}) = d/2$, the solution is

$$\lambda_{\mathrm{SC}} = \frac{d}{2}\left\{1 - \frac{\gamma'}{\gamma}\left[1 - \left(\frac{t}{\tau_{\mathrm{sep}}}\right)^{1/4}\right]\right\}. \tag{37}$$

The electric field can then be calculated using Eq. (26), resulting in

$$E_{\mathrm{SC}} = \sqrt{\frac{\frac{d}{2}-x}{\lambda_{\mathrm{SC}}}E_{\mathrm{bulk}}^2 + \frac{x+\lambda_{\mathrm{SC}}-\frac{d}{2}}{\lambda_{\mathrm{SC}}}E_{\mathrm{int}}^2}, \tag{38}$$

in which $E_{\mathrm{int}}(t)$ is the electric field at the interface between the space charge region and the surface charge

$$E_{\mathrm{int}} = \frac{V_A}{d}\sqrt{\left(\frac{E_{\mathrm{bulk}}}{V_A/d}\right)^2 + \frac{9}{2\gamma}\frac{E_{\mathrm{bulk}}}{V_A/\lambda_{\mathrm{SC}}}}. \tag{39}$$

Using Eqs. (17) and (39), and using the assumption of a homogeneous current density, we find the following expression for n_{SC}:

$$n_{\mathrm{SC}} = \frac{1}{\sqrt{\frac{\frac{d}{2}-x}{\lambda_{\mathrm{SC}}}\frac{1}{(2\bar{n})^2} + \frac{x+\lambda_{\mathrm{SC}}-\frac{d}{2}}{\lambda_{\mathrm{SC}}}\frac{1}{n_{\mathrm{int}}^2}}}, \tag{40}$$

in which $n_{\mathrm{int}}(t)$ is the concentration at the interface between the space charge region and the surface charge

$$n_{\mathrm{int}} = 2\bar{n}\frac{E_{\mathrm{bulk}}}{E_{\mathrm{int}}}. \tag{41}$$

In Fig. 3, this analytical description is compared with simulation results for $\tilde{Q}_{\mathrm{tot}}=10^6$ and $\tilde{V}_A=10^3$, a representative situation for the space charge limited regime. As with the geometry limited regime, we see that the dynamics are described well by the theory, although diffusion smears out the sharp variations. Figure 3 also justifies the assumption of a homogeneous current density.

The surface charge Q_s during the depletion phase can be calculated by taking the difference between the total charge and the integral of the concentration in Eq. (15), using Eq. (40): $Q_s = 2q\bar{n}\lambda_{\mathrm{SC}}[1-2n_{\mathrm{int}}/(n_{\mathrm{int}}+2\bar{n})]$. As in Sec. II A 2, we introduce diffusion to find a more detailed description of the concentration and the electric field close to the electrodes. The charge near the electrode is then not described by a surface charge anymore, but forms a very narrow double layer. Using the approximation that is close to the electrodes only one polarity of charges is present, we can write Eq. (3) as $J = \mu\rho E - D\,\partial\rho/\partial x$. We assume that the charges in the double layer are already in the steady state distribution, so the integral of this equation over any interval within this

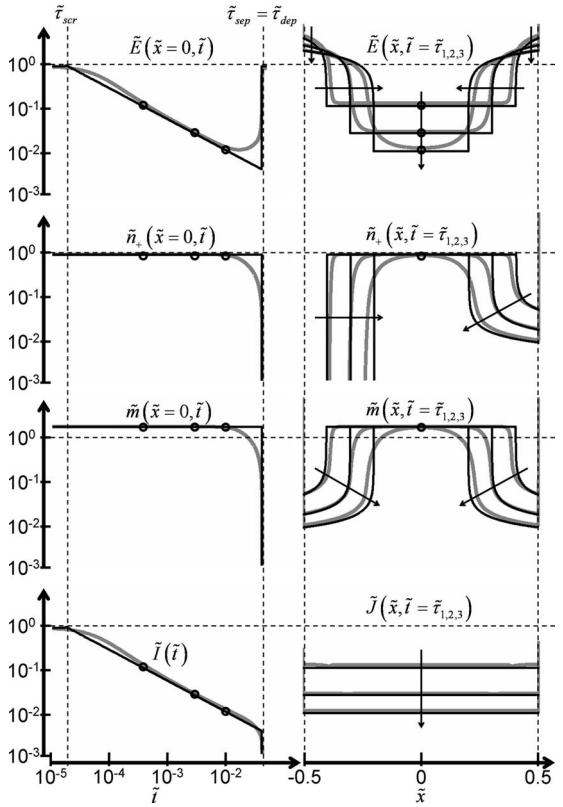

FIG. 3. Comparison between theory (black curves) and simulation (gray curves) for $\tilde{Q}_{\mathrm{tot}}=10^6$ and $\tilde{V}_A=1000$ (representative for the space charge limited regime). Where the gray curves are not visible, they are coinciding with the black curves. On the left, the electric field, the concentration of positive charges and the total concentration in the middle of the device, as well as the external current, are shown in function of time. On the right, the electric field, the concentration of positive charges, the total concentration and the current density are shown in function of place at times $\tilde{\tau}_1=0.000\,35$, $\tilde{\tau}_2=0.0025$, and $\tilde{\tau}_3=0.009\,35$. The dots on the left indicate these three times, the dots on the right indicate the position from the corresponding curves on the left.

double layer is zero. Using Eq. (2) and neglecting diffusion outside the double layer, this results in $E_{\mathrm{DL}}^2-2V_T\partial E_{\mathrm{DL}}/\partial x=E_{\mathrm{int}}^2$, in which $E_{\mathrm{DL}}(x,t)$ is the electric field in the double layer near the negative electrode. A similar differential equation arises in the solution of the steady state situation of this regime, and is solved in [26]. Using the same method, the solution is

$$E_{\mathrm{DL}}=E_{\mathrm{int}}\coth\left[\frac{E_{\mathrm{int}}}{2V_T}\left(\frac{d}{2}-x\right)+\operatorname{arc\,tanh}\left(\frac{E_{\mathrm{int}}}{E_{\mathrm{el}}}\right)\right], \quad (42)$$

in which $E_{\mathrm{el}}(t)$ is the electric field at the electrode:

$$E_{\mathrm{el}}=E_{\mathrm{int}}+\frac{Q_s}{\epsilon\epsilon_0}. \quad (43)$$

The concentration in the double layer can be found using Gauss's equation, resulting in

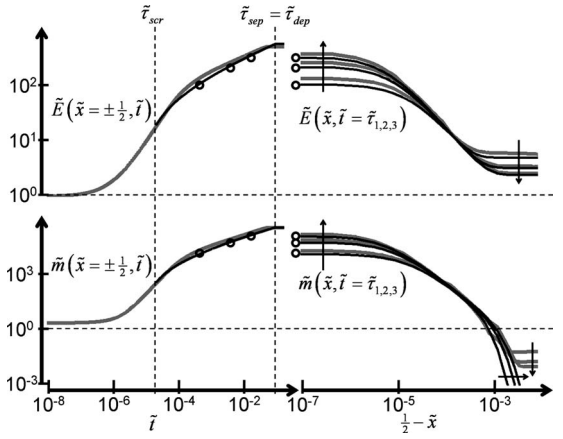

FIG. 4. Comparison between theory (black curves) and simulation (gray curves) for $\tilde{Q}_{\mathrm{tot}}=10^6$ and $\tilde{V}_A=1000$ (representative for the space charge limited regime). Where the gray curves are not visible, they are coinciding with the black curves. On the left, the electric field and total concentration at the electrode are shown in function of time. On the right, the electric field and total concentration in the double layer are shown in function of place at times $\tilde{\tau}_1=0.000\,35$, $\tilde{\tau}_2=0.0025$, and $\tilde{\tau}_3=0.009\,35$. The dots on the left indicate these three times, the dots on the right indicate the position from the corresponding curves on the left.

$$n_{\mathrm{DL}}=\frac{\epsilon\epsilon_0E_{\mathrm{int}}^2}{2qV_T}\operatorname{csch}^2\left[\frac{E_{\mathrm{int}}}{2V_T}\left(\frac{d}{2}-x\right)+\operatorname{arc\,tanh}\left(\frac{E_{\mathrm{int}}}{E_{\mathrm{el}}}\right)\right]. \quad (44)$$

Equations (42) and (44) agree very well with numerical results (Fig. 4).

B. Regimes with diffusion

When the applied voltage is low, diffusion is the dominant transport mechanism. However, even for very low voltages, drift cannot be completely neglected, otherwise the distribution of charges in the device would always remain homogeneous. Therefore, we have to use the full Nernst-Planck equation in Eq. (3), which can be combined with the continuity Eq. (4) to give

$$\frac{1}{D}\frac{\partial n_\pm}{\partial t}=\mp\frac{1}{V_T}\frac{\partial}{\partial x}(n_\pm E)+\frac{\partial^2 n_\pm}{\partial x^2}. \quad (45)$$

The boundary conditions can be written as $V_T\partial n_\pm/\partial x|_{-d/2}=\pm E(-d/2,t)n_\pm(-d/2,t)$ and $V_T/\partial x|_{d/2}=\pm E(d/2,t)\times n_\pm(d/2,t)$. In the regimes with diffusion, discrete surface charge does not appear. We will, as in Sec. II A, discuss two limiting cases in which the electric field is either almost homogeneous (in the diffusion limited regime) or almost completely screened (in the double layer limited regime).

1. Diffusion limited regime

As in Sec. II A 1, we will replace Eq. (1) and (2) by $E=V_A/d$, so Eq. (45) becomes

$$\frac{1}{D}\frac{\partial n_{\pm}}{\partial t} = \mp \frac{\tilde{V}_A}{d}\frac{\partial n_{\pm}}{\partial x} + \frac{\partial^2 n_{\pm}}{\partial x^2}. \tag{46}$$

The steady state distributions $n_{\pm,\mathrm{SS}}(x)$ can then be found by setting the time derivative in Eq. (46) zero, resulting in

$$n_{\pm,\mathrm{SS}} = \bar{n}\frac{\tilde{V}_A}{2}\mathrm{csch}\left(\frac{\tilde{V}_A}{2}\right)e^{\pm \tilde{V}_A x/d}. \tag{47}$$

The dynamic solution for this regime can be derived using standard separation of variables techniques [29] and yields

$$n_{\pm} = n_{\pm,\mathrm{SS}}\left(1 + \frac{1}{\tilde{V}_A}e^{\tilde{V}_A/2(1/2\mp x/d)} \times \sum_{i=1}^{\infty} C_i X_{\pm,i} e^{-\tilde{V}_A^2/4(1+4i^2\pi^2/\tilde{V}_A^2)D/d^2 t}\right), \tag{48}$$

with

$$X_{\pm,i} = \frac{2i\pi}{\tilde{V}_A}\cos\left(i\frac{\pi}{2} \pm \frac{i\pi x}{d}\right) + \sin\left(i\frac{\pi}{2} \pm \frac{i\pi x}{d}\right), \tag{49}$$

$$C_i = 8\frac{\frac{2i\pi}{\tilde{V}_A}}{\left(1 + \frac{4i^2\pi^2}{\tilde{V}_A^2}\right)^2}[(-1)^i e^{-\tilde{V}_A/2} - 1]. \tag{50}$$

For low $\tilde{V}_A$, $n_{\pm}$ can be approximated as

$$n_{\pm} = \bar{n}\left(1 \pm \tilde{V}_A\frac{x}{d}\right) \mp \frac{4\tilde{V}_A\bar{n}}{\pi^2}\sum_{i=1}^{\infty}\frac{1}{i^2}\sin\left(i\frac{\pi}{2}\right)\sin\left(\frac{x}{d}i\pi\right)e^{-i^2\pi^2 D/d^2 t}, \tag{51}$$

from which it is clear that the steady state solution is reached for $t \to \infty$. Using the expansion of the steady state solution

$$\bar{n}\left(1 \pm \tilde{V}_A\frac{x}{d}\right) = \bar{n}\left[1 \pm \frac{4\tilde{V}_A}{\pi^2}\sum_{i=1}^{\infty}\frac{1}{i^2}\sin\left(i\frac{\pi}{2}\right)\sin\left(\frac{x}{d}i\pi\right)\right]. \tag{52}$$

Equation (51) can also be written as

$$n_{\pm} = \bar{n} \pm \frac{4\tilde{V}_A\bar{n}}{\pi^2}\sum_{i=1}^{\infty}\frac{1}{i^2}\sin\left(i\frac{\pi}{2}\right)\sin\left(\frac{x}{d}i\pi\right)(1 - e^{-i^2\pi^2 D/d^2 t}), \tag{53}$$

in which it is clear that $n_{\pm} = \bar{n}$ at $t=0$, as we expect. Using Eq. (6), the external current can be calculated as

$$I = I_0\frac{8}{\pi^2}\sum_{i=1,3,5,\ldots}\frac{1}{i^2}e^{-i^2\pi^2 D/d^2 t}. \tag{54}$$

With the identity $\pi^2/8 = \Sigma_{i=1,3,5,\ldots} i^{-2}$ it becomes clear that, for $t=0$, $I=I_0$, as expected.

As time progresses, the term for $i=1$ becomes very quickly dominant in Eqs. (51) and (54), and in this case we can write

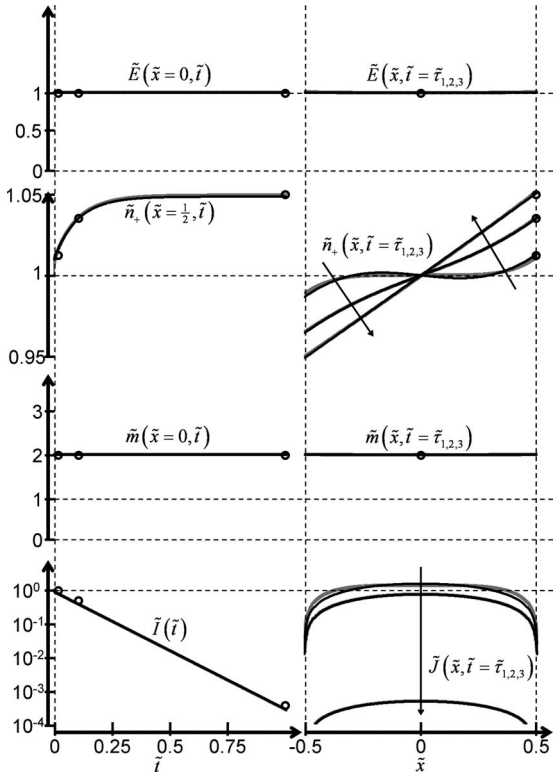

FIG. 5. Comparison between theory (black curves) and simulation (gray curves) for $\tilde{Q}_{\mathrm{tot}}=0.1$ and $\tilde{V}_A=0.1$ (representative for the diffusion limited regime). Where the gray curves are not visible, they are coinciding with the black curves. On the left, the electric field in the middle of the device, the concentration of positive charges at the electrode and the total concentration in the middle of the device, as well as the external current, are shown in function of time. On the right, the electric field, the concentration of positive charges, the total concentration and the current density are shown in function of place at times $\tilde{\tau}_1=0.01$, $\tilde{\tau}_2=0.1$, and $\tilde{\tau}_3=1$. The dots on the left indicate these three times, the dots on the right indicate the position from the corresponding curves on the left.

$$n_{\pm} = \bar{n}\left(1 \pm \tilde{V}_A\frac{x}{d}\right) \mp \frac{4\tilde{V}_A\bar{n}}{\pi^2}\sin\left(\frac{x}{d}\pi\right)e^{-\pi^2 D/d^2 t}, \tag{55}$$

$$I = I_0\frac{8}{\pi^2}e^{-\pi^2 D/d^2 t}. \tag{56}$$

From Eq. (55), we can conclude that $m=2\bar{n}$. The fact that the total concentration is homogeneous is typical for the regimes in which diffusion is a limiting factor, as we will see in the next paragraph.

Figure 5 shows a comparison between the theoretical description of the diffusion limited regime and simulation results for $\tilde{Q}_{\mathrm{tot}}=\tilde{V}_A=0.1$, which are representative values for this regime. Except at very small times, when neglect of the higher order harmonics leads to small differences, the theoretical description agrees very well with the numerical results. It is clear that the electric field and the total concentration are indeed homogeneous and constant.

2. Double layer limited regime

When the applied voltage is low and the charge content is high, both diffusion and screening are important. The limiting regime under these circumstances has been solved in Refs. [19] and [1]. Our aim in this paper is to show that, using a similar approach as for the other regimes discussed in this paper, we can arrive at the same conclusions. In the space charge limited regime, the fact that screening is a limiting mechanism leads to the assumption of a homogeneous current density J. In the diffusion limited regime, it was found that the total concentration m is homogeneous. In the regime of low voltage and high concentration, both screening and diffusion are limiting mechanisms, and we can combine the two assumptions $\partial J/\partial x=0$ and $m=2\bar{n}$. Using Eqs. (2) and (3), we find then

$$J = 2q\bar{n}\mu\left(E - \lambda_{\mathrm{DL}}^2\frac{\partial^2 E}{\partial x^2}\right), \tag{57}$$

in which the double layer length (or the Debye length) λ_{DL} is defined as

$$\lambda_{\mathrm{DL}} = \sqrt{\frac{\epsilon\epsilon_0 V_T}{2q\bar{n}}}. \tag{58}$$

The steady state solution $E_{\mathrm{ss}}(x)$ of the electric field can be found by setting the current density in Eq. (57) zero, and using Eq. (1) and the fact that the electric field is symmetric around $x=0$:

$$E_{\mathrm{ss}} = \frac{V_A}{d}\frac{d}{2\lambda_{\mathrm{DL}}}\mathrm{csch}\left(\frac{d}{2\lambda_{\mathrm{DL}}}\right)\cosh\left(\frac{x}{\lambda_{\mathrm{DL}}}\right). \tag{59}$$

Using Eq. (2), we find $\rho_{\mathrm{ss}}(x)$, the steady state solution of the charge density

$$\rho_{\mathrm{ss}} = q\bar{n}\tilde{V}_A\mathrm{csch}\left(\frac{d}{2\lambda_{\mathrm{DL}}}\right)\sinh\left(\frac{x}{\lambda_{\mathrm{DL}}}\right). \tag{60}$$

Taking the derivative of Eq. (57) with respect to x, and using Eq. (2) and the assumption of a homogeneous current density, we obtain $\rho=\lambda_{\mathrm{DL}}^2\partial^2\rho/\partial x^2$. Using Eq. (60), we can see that the transient part $\rho_{\mathrm{tr}}(x,t)$ of the charge density, defined as $\rho_{\mathrm{tr}}=\rho-\rho_{\mathrm{ss}}$, is also a solution of this differential equation $\rho_{\mathrm{tr}}=\lambda_{\mathrm{DL}}^2\partial^2\rho_{tr}/\partial x^2$. Using the fact that ρ has to be antisymmetric around $x=0$, the solution of this differential equation is

$$\rho_{\mathrm{tr}} = C\sinh\left(\frac{x}{\lambda_{\mathrm{DL}}}\right), \tag{61}$$

in which $C(t)$ is an integration constant that can be found by calculating the external current using two different methods.

For the first method, we use Eqs. (1) and (2) to find the electric field

$$E = E_{\mathrm{ss}} + \frac{\lambda_{\mathrm{DL}}}{\epsilon\epsilon_0}C\left[\cosh\left(\frac{x}{\lambda_{\mathrm{DL}}}\right) - \frac{2\lambda_{\mathrm{DL}}}{d}\sinh\left(\frac{d}{2\lambda_{\mathrm{DL}}}\right)\right], \tag{62}$$

which we can use in Eq. (5) to find an expression for the external current

$$I = \lambda_{\mathrm{DL}}\frac{dC}{dt}\left[\cosh\left(\frac{d}{2\lambda_{\mathrm{DL}}}\right) - \frac{2\lambda_{\mathrm{DL}}}{d}\sinh\left(\frac{d}{2\lambda_{\mathrm{DL}}}\right)\right]. \tag{63}$$

For the second method, we calculate the current density J using Eqs. (57) and (62):

$$J = -C\frac{2D}{d}\sinh\left(\frac{d}{2\lambda_{\mathrm{DL}}}\right). \tag{64}$$

Since the current density is homogeneous, Eq. (6) shows that it has to be equal to the external current, so the right-hand sides in Eqs. (63) and (64) have to be equal:

$$\left[\coth\left(\frac{d}{2\lambda_{\mathrm{DL}}}\right) - \frac{2\lambda_{\mathrm{DL}}}{d}\right]\frac{dC}{dt} = -\frac{2D}{\lambda_{\mathrm{DL}}d}C. \tag{65}$$

Since at $t=0$, the transient part of the charge density has to compensate the steady state part, we can write $C(0)=-q\bar{n}\tilde{V}_A\mathrm{csch}(\frac{1}{2}d/\lambda_{\mathrm{DL}})$. The solution of Eq. (65), using this initial condition, is

$$C = -q\bar{n}\tilde{V}_A\,\mathrm{csch}\left(\frac{d}{2\lambda_{\mathrm{DL}}}\right)e^{-t/\tau_{\mathrm{DL}}}. \tag{66}$$

in which τ_{DL} (s) is the time constant of the double layer regime

$$\tau_{\mathrm{DL}} = \left[\coth\left(\frac{d}{2\lambda_{\mathrm{DL}}}\right) - \frac{2\lambda_{\mathrm{DL}}}{d}\right]\frac{\lambda_{\mathrm{DL}}d}{2D}, \tag{67}$$

which reduces, for $\lambda_{\mathrm{DL}}\ll d$, to $\tau_{\mathrm{DL}}=\frac{1}{2}\lambda_{DL}d/D$. The charge concentration and electric field are then

$$\rho = \rho_{\mathrm{ss}}(1 - e^{-t/\tau_{\mathrm{DL}}}), \tag{68}$$

$$E = \frac{V_A}{d}e^{-t/\tau_{\mathrm{DL}}} + E_{\mathrm{ss}}(1 - e^{-t/\tau_{\mathrm{DL}}}). \tag{69}$$

The external current can be calculated using Eqs. (64) and (66):

$$I = I_0 e^{-t/\tau_{\mathrm{DL}}}. \tag{70}$$

The comparison, in Fig. 6, between the theoretical description of the double layer limited regime and numerical results for the representative situation $\tilde{Q}_{\mathrm{tot}}=10^6$ and $\tilde{V}_A=0.1$, justifies the assumption that the total concentration is constant and homogeneous. The other quantities are only nonhomogeneous in the double layer close to the electrodes. The assumption of a homogeneous current density does not hold near the electrodes, but the variation occurs over such a small layer that the external current is still described very well by Eq. (70).

III. APPLICABILITY OF THE REGIMES

A. Comparison between theory and simulation

To investigate in which regions of the $(\tilde{V}_A,\tilde{Q}_{\mathrm{tot}})$ parameter-plane the respective regimes are applicable, we have performed over 20000 simulations covering the plane. For each simulation, we calculate one value for each regime,

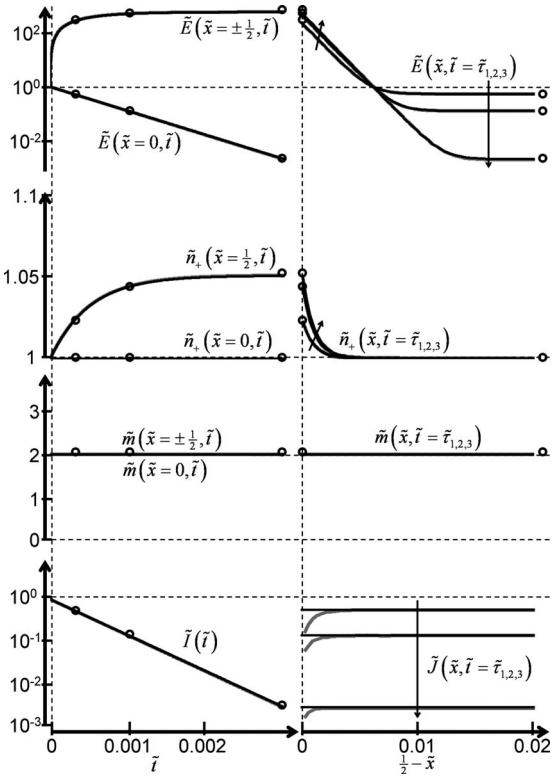

FIG. 6. Comparison between theory (black curves) and simulation (gray curves) for $\tilde{Q}_{\mathrm{tot}}=10^6$ and $\tilde{V}_A=0.1$ (representative for the double layer limited regime). Where the gray curves are not visible, they are coinciding with the black curves. On the left, the electric field, the concentration of positive charges and the total concentration in the middle of the device and at the electrode, as well as the external current, are shown in function of time. On the right, the electric field, the concentration of positive charges, the total concentration and the current density are shown in function of place near the electrode at times $\tilde{\tau}_1=0.0003$, $\tilde{\tau}_2=0.001$, and $\tilde{\tau}_3=0.003$. The dots on the left indicate these three times, the dots on the right indicate the position from the corresponding curves on the left.

which is a measure for the difference between the simulation and the theory. Representing the time and place dependent dynamics by one value is arbitrary, and for different aspects of the dynamics different regions in the $(\tilde{V}_A,\tilde{Q}_{\mathrm{tot}})$ parameter plane will be described well by the theory. Therefore, the aim of this paragraph is to obtain a general idea of the applicability of the theoretical descriptions of the four regimes.

As a place-independent quantity which represents the dynamics of the device for a particular point in the $(\tilde{V}_A,\tilde{Q}_{\mathrm{tot}})$ parameter plane, we choose the external current I. For each regime, we calculate $\Delta(\tilde{V}_A,\tilde{Q}_{\mathrm{tot}})$, the normalized root mean square error between the simulated and the theoretical current, with the following formula:

$$\Delta=\frac{1}{I_{\mathrm{sim}}(0)}\sqrt{\frac{\int_{t_{90\%}}^{t_{10\%}}(I_{\mathrm{sim}}-I_{\mathrm{th}})^2dt}{t_{10\%}-t_{90\%}}}. \tag{71}$$

In this formula, $t_{90\%}$ and $t_{10\%}$ are the times for which the simulated current I_{sim} reaches 90% and 10% of its initial value $I_{\mathrm{sim}}(0)$. I_{th} is the theoretical current which can be calculated for the four regimes, using Eqs. (23), (35), (56), and (70). Depending on which equation we choose, we obtain the values Δ_{GL} for the geometry limited regime, Δ_{SCL} for the space charge limited regime, Δ_{DL} for the diffusion limited regime or Δ_{DLL} for the double layer limited regime.

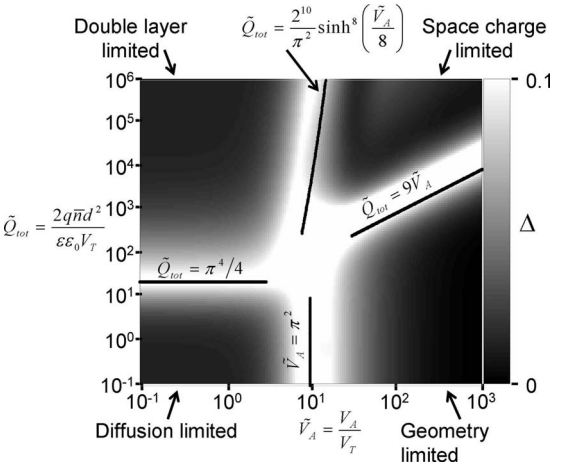

FIG. 7. The relative error between theory and simulation in the $(\tilde{V}_A,\tilde{Q}_{\mathrm{tot}})$ parameter plane. A darker shade corresponds to a better agreement. The four different regimes and the borders between them are indicated.

Figure 7 shows the smallest of these four values for all of the performed simulations on the $(\tilde{V}_A,\tilde{Q}_{\mathrm{tot}})$ parameter plane. We can clearly see the four regions which correspond to the four regimes. As expected, the geometry limited regime is applicable for small $\tilde{Q}_{\mathrm{tot}}$ and large $\tilde{V}_A$, the space charge limited regime for large $\tilde{Q}_{\mathrm{tot}}$ and $\tilde{V}_A$, the diffusion limited regime for small $\tilde{Q}_{\mathrm{tot}}$ and $\tilde{V}_A$, and the double layer limited regime for large $\tilde{Q}_{\mathrm{tot}}$ and small $\tilde{V}_A$.

B. Borders between the regimes

It is useful to have a "rule of thumb" to determine quickly which regime describes best the situation for a particular combination of values for $\tilde{Q}_{\mathrm{tot}}$ and $\tilde{V}_A$. In order to find such rules we will compare the different time constants which are typical for the different regimes.

The time constants $\tau_{\mathrm{dep}}=d^2/(\mu V_A)$ in the geometry limited regime, $\tilde{\tau}_{\mathrm{DL}}=d\lambda_{\mathrm{DL}}/(2D)$ in the double layer limited regime, and $d^2/(\pi^2 D)$ in the diffusion limited regime all represent the initial slope of the external current. τ_{dep} becomes equal to $d^2/(\pi^2 D)$ for $\tilde{V}_A=\pi^2\approx 10$, which is plotted in Fig. 7 and can be seen to be a useful rule to distinguish between the geometry limited and the diffusion limited regime. Similarly, τ_{DL} is equal to $d^2/(\pi^2 D)$ for $\tilde{Q}_{\mathrm{tot}}=\pi^4/4\approx 25$, which turns out to be a useful border between the diffusion limited and the double layer limited regime. To obtain a border between the geometry limited regime and the space charge limited regime, we compare the separation times τ_{sep}, which are given by $d^2/(2\mu V_A)$ and Eq. (30), respectively. They are equal for $\tilde{Q}_{\mathrm{tot}}=9\tilde{V}_A$, which is also plotted in Fig. 7.

A rule for the border between the space charge limited and the double layer limited regimes is not so easy to obtain because there are no time constants that have a similar meaning in both regimes. In Ref. [1], two intermediate regimes between the double layer limited regime (which is referred to as the 'linear' regime) and the space charge limited regime are discussed. The "weakly nonlinear" regime describes the situation in which the total concentration can still be considered constant in the bulk (as in the double layer limited regime), but not near the electrodes. The "strongly nonlinear" regime describes the situation in which space charge layers are formed (as in the space charge limited regime), but the electric field is still mostly screened by the double layers. The criterium used in Ref. [1] to distinguish between these two intermediary regimes is $\tilde{Q}_{\mathrm{tot}}=(2^{10}/\pi^2)\sinh^8(\tilde{V}_A/8)$. In Fig. 7, we can see that this criterion is also useful as a border between the double layer limited and the space charge limited regimes.

IV. CURRENT MEASUREMENTS

We illustrate and validate the general analytical description, which is relevant for a broad range of applications, by experiments on one particular material system. Mixtures of nonpolar liquids and surfactants allow a good control of the charge content over several decades. The low reactivity, both in the bulk and at the electrodes, allows an almost complete depletion of charges, and prevents generation currents to dominate the electrical behavior. For these reasons, these mixtures act as a model system for the problem discussed in this work.

The devices used for the transient current measurements consist of two glass plates, both coated with a transparent ITO electrode of 1 cm^2. Spacer balls hold these two electrodes separated at a distance d. The space between the electrodes is filled with a mixture of high purity (99.9%) n-dodecane ($\epsilon=2$) (Aldrich) and OLOA 1200, a 50% mineral oil containing surfactant polyisobutylene succinimide (Chevron) [30]. The surfactant molecules form inverse micelles, which can disproportionate resulting in a symmetric 1:1 electrolyte [14,15]. The concentration of charged inverse micelles $\bar{n}$ is proportional with the weight percentage of surfactant in the mixture, with a proportionality constant of roughly 5×10^{19} m^{-3} per wt % [14].

Five devices with different thicknesses and concentrations of surfactant have been made. The exact thickness of each device was obtained by measuring the capacitance of the device before filling. Table I gives an overview of the properties of the different devices. They are chosen in such a way that the resulting values for $\tilde{Q}_{\mathrm{tot}}$ cover a large interval in Figs. 7 and 8.

TABLE I. Properties of the five devices used for the measurements shown in this work.

Device number	Surfactant concentration (wt %)	Expected $\bar{n}$ (m^{-3})	Measured d (μm)	Estimated $\tilde{Q}_{\mathrm{tot}}$ (no unit)
1	0.01	5.0×10^{17}	2.2	1.75
2	0.03	1.5×10^{18}	4.5	22
3	0.10	5.0×10^{18}	9.4	320
4	0.30	1.5×10^{19}	14.8	2380
5	1.00	5.0×10^{19}	26.8	26000

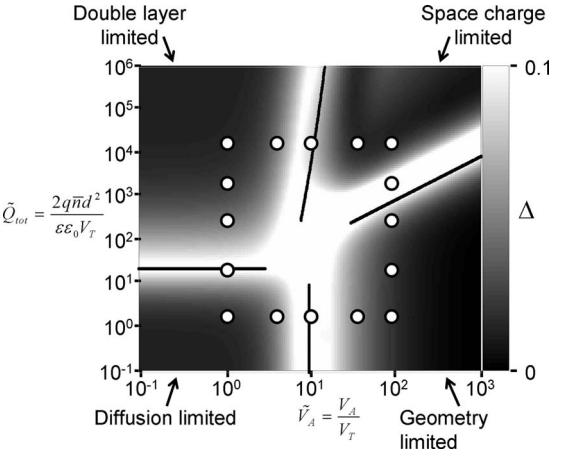

FIG. 8. Location of the $(\tilde{V}_A,\tilde{Q}_{\mathrm{tot}})$ parameters of the measurements shown in this work, in the $(\tilde{V}_A,\tilde{Q}_{\mathrm{tot}})$ parameter plane.

Before every measurement, the devices are short circuited for a sufficient amount of time to ensure a homogeneous distribution of charges. Then the voltage is abruptly changed to V_A and the resulting external transient current is measured. These measurements were performed for voltages of 25 mV, 100 mV, 250 mV, 1 V, and 2.5 V. Figure 8 shows the location in the $(\tilde{V}_A,\tilde{Q}_{\mathrm{tot}})$ parameter-plane of all the measurements shown in this section.

A. Low voltages

The currents, measured when a voltage of 25 mV is applied on each of the five devices, are shown in Fig. 9. The concentration $\bar{n}$ and the mobility μ of the charges have been estimated by fitting simulations to these measurements. The best fits are included in Fig. 9, and are found for the values listed in the first columns of Tables II and III. The values for the concentration are consistent with the expected values.

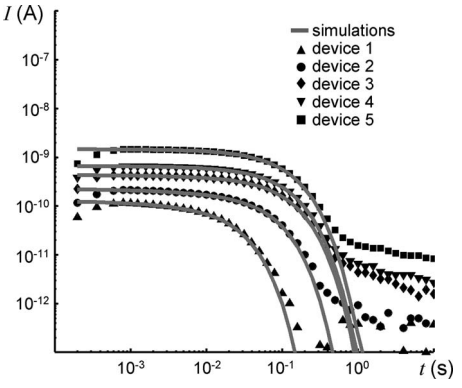

FIG. 9. Current measurements and numerical fit for the five devices in Table I, when a voltage step from 0 V to 25 mV is applied.

TABLE II. Average concentration of charges, estimated by numerical fitting (for the five devices), by applying Eq. (72) at 2.5 V (for the five devices), and by fitting with the analytical expressions in each of the four regimes (only for devices 1 and 5).

	$\hat{\bar{n}}$ (m^{-3})			
Device	Numerical fit with simulation	Using Eq. (72)	Theoretical fit for high voltage	Theoretical fit for low voltage
1	4.3×10^{17}	3.5×10^{17}	4.2×10^{17}	4.1×10^{17}
2	1.3×10^{18}	1.3×10^{18}		
3	6.6×10^{18}	6.6×10^{18}		
4	1.4×10^{19}	1.5×10^{19}		
5	7.2×10^{19}	6.2×10^{19}	8.5×10^{19}	7.8×10^{19}

Also the values for the mobility agree well with the results in other works [14,19,20].

The good agreement between the measurements and the simulations in Fig. 9 and in the following paragraphs, indicates that the dynamics of the devices during the transient phase can be modeled well by drift, diffusion and screening, as described by the Poisson-Nernst-Planck equations. The deviations at very short times are a result of the charging time of the measurement setup. At large times, other effects, such as the generations of new charged inverse micelles [14] and reactions at the electrodes, become important, resulting in a current even when the transient phase is finished.

B. High voltages

The currents, measured when a voltage of 2.5 V is applied on each of the five devices, are shown in Fig. 10, together with the corresponding simulations for the parameters found in the previous paragraph. At high voltages, we can, however, estimate the concentration and the mobility more easily by using the fact that positive and negative charges become completely separated [19,20,28]. We can then use Eqs. (7) and (21) to find

TABLE III. Mobility of the charges, estimated by numerical fitting (for the five devices), by applying Eq. (73) at 2.5 V (for the five devices), and by fitting with the analytical expressions in each of the four regimes (only for devices 1 and 5).

	$\hat{\mu}$ ($m^2\ V^{-1}\ s^{-1}$)			
Device	Numerical fit with simulation	Using Eq. (73)	Theoretical fit for high voltage	Theoretical fit for low voltage
1	8.8×10^{-10}	7.1×10^{-10}	8.5×10^{-10}	8.6×10^{-10}
2	9.8×10^{-10}	8.7×10^{-10}		
3	8.0×10^{-10}	7.0×10^{-10}		
4	9.0×10^{-10}	8.1×10^{-10}		
5	7.0×10^{-10}	8.1×10^{-10}	5.9×10^{-10}	6.4×10^{-10}

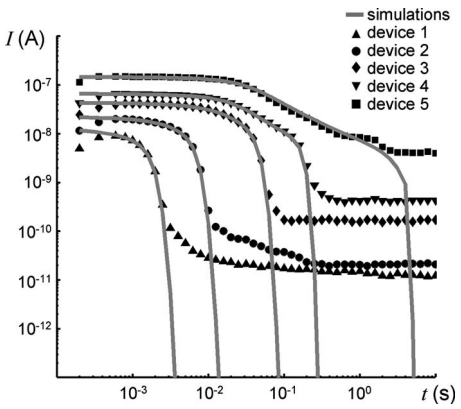

FIG. 10. Current measurements and numerical fit for the five devices in Table I, when a voltage step from 0 V to 2.5 V is applied.

$$\hat{\bar{n}} = \frac{1}{qdS}\widehat{\int_0^{\tau_{\mathrm{dep}}} I dt}, \tag{72}$$

$$\hat{\mu} = \frac{d^2}{2V_A}\hat{I}_0\widehat{\left(\int_0^{\tau_{\mathrm{dep}}} I dt\right)^{-1}}. \tag{73}$$

The hats denote estimations of the corresponding quantities. The integrals in these equations are only calculated until the end of the transient at the depletion time, which can be easily estimated from the measurements, to avoid including the current as a result from reactions in the bulk or at the electrodes. In estimating the initial current, an extrapolation has to be made to take into account the charging time of the measurement setup.

Applying this estimation to the measurements of Fig. 10 results in the values shown in the second column of Tables II and III. The good agreement with the values obtained from the fit with simulations demonstrates that the assumption of a complete separation of charges is justified.

C. Low charge content

Figure 11 shows the measured currents, together with the fitted simulation, for the device with the lowest $\tilde{Q}_{\mathrm{tot}}$ (device

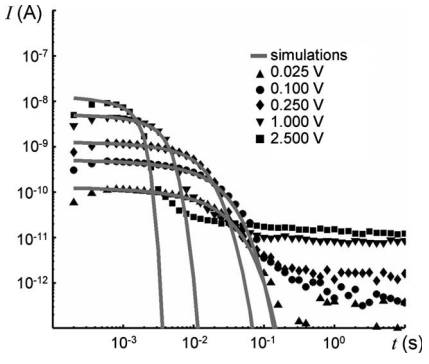

FIG. 11. Current measurements and numerical fit for device 1 (with the lowest charge content), when a voltage step from 0 V to five different voltages is applied.

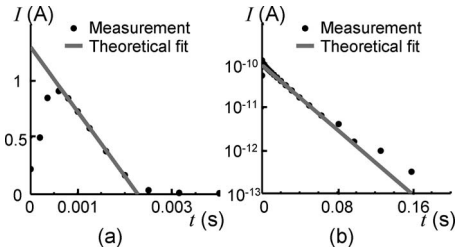

FIG. 12. Fit between theory and measurement for device 1 (with the lowest charge content), when (a) a voltage step from 0 V to 2.5 V is applied (the geometry limited regime) and (b) a voltage step from 0 V to 25 mV is applied (the diffusion limited regime).

1), and for five different voltages. On Fig. 8 we can see that for the lowest voltage the diffusion limited regime should apply, while for the highest voltage the geometry limited regime should apply. Therefore we can fit the derived expressions for the current with the measurements to find the concentration and the mobility.

For the measurement at 2.5 V we find the best linear fit of the form $-\hat{A}t+\hat{B}$, shown in Fig. 12(a). Using Eq. (23), the concentration and the mobility can then be calculated as

$$\hat{\tilde{n}} = \frac{1}{2qdS}\frac{\hat{B}^2}{\hat{A}}, \tag{74}$$

$$\hat{\mu} = \frac{d^2}{V_A}\frac{\hat{A}}{\hat{B}}. \tag{75}$$

The results for device 1 are also listed in Tables II and III.

For the measurement at 25 mV we find the best exponential fit of the form $I=\hat{C}\exp(-\hat{D}t)$, shown in Fig. 12(b). Using Eq. (56), the concentration and the mobility can then be calculated as

$$\hat{\tilde{n}} = \frac{\pi^4 kT}{16q^2 dV_A S}\frac{\hat{C}}{\hat{D}}, \tag{76}$$

$$\hat{\mu} = \frac{qd^2}{\pi^2 kT}\hat{D}. \tag{77}$$

The results for device 1 are listed in Tables II and III. The good agreement between all estimations for the mobility and the concentration indicates the validity of the theoretical approximations.

It should be noted that for the above estimations we have to know the charge q of the charged inverse micelles. However, by combining the measurements at high and at low voltages, we can also estimate this charge. Using Eqs. (75) and (77), we find

$$\hat{q} = \frac{\pi^2 kT}{V_A}\frac{\hat{A}}{\hat{B}\hat{D}}. \tag{78}$$

For our measurements, this results in a charge of 1.58×10^{-19} C, which confirms the results in other works [14,26] that the valency of the charges in the mixture used in this work is 1.

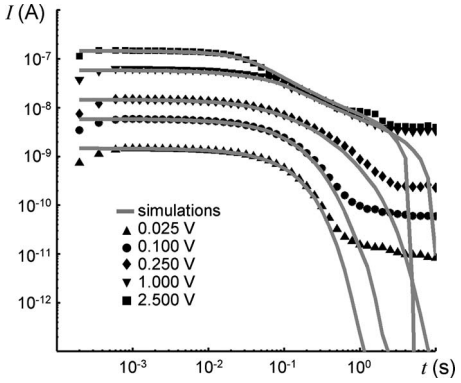

FIG. 13. Current measurements and numerical fit for device 5 (with the highest charge content), when a voltage step from 0 V to five different voltages is applied.

D. High charge content

The measured currents at five different voltages for the device with the highest $\tilde{Q}_{\text{tot}}$ (device 5), are shown, together with the simulations, in Fig. 13. Figure 8 shows that in this case for the lowest voltage the double layer limited regime should apply and for the highest voltage the space charge limited regime.

Similarly as in the previous paragraph, we can compare the measurements with the theoretical expressions for the current to estimate the mobility and the concentration. For the space charge limited regime however, this results in impractical expressions. In this case, it is much easier to find the best fit between the measurement at 2.5 V and Eq. (35) graphically or numerically. This fit is found for the values listed in Tables II and III, and is shown in Fig. 14(a).

For the measurement at the lowest voltage, we find the best exponential fit of the form $I=\hat{C}\exp(-\hat{D}t)$, shown in Fig. 14(b). Using Eq. (70), we can estimate the concentration and the mobility as

$$\hat{\tilde{n}} = \frac{2kT}{\epsilon\epsilon_0 q^2 V_A^2 S^2}\frac{\hat{C}^2}{\hat{D}^2}, \tag{79}$$

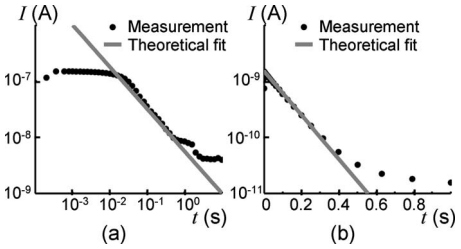

FIG. 14. Fit between theory and measurement for device 5 (with the highest charge content), when (a) a voltage step from 0 V to 2.5 V is applied (the space charge limited regime) and (b) a voltage step from 0 V to 25 mV is applied (the double layer limited regime).

$$\hat{\mu} = \frac{qV_A S\epsilon\epsilon_0 d}{4kT}\frac{\hat{D}^2}{\hat{C}}. \tag{80}$$

The resulting values for device 5 are listed in Tables II and III.

Also for this device with high $\tilde{Q}_{\mathrm{tot}}$ we can estimate the charge q. Now we combine Eq. (73) (for the measurement at the highest voltage) and Eq. (80) (for the measurement at the lowest voltage), to find

$$\hat{q} = \frac{2kTd}{\epsilon\epsilon_0 S V_{A,\mathrm{low}} V_{A,\mathrm{high}}}\frac{\hat{C}}{\hat{D}^2}\hat{I}_0\overbrace{\left(\int_0^{\tau_{\mathrm{dep}}} Idt\right)^{-1}}. \tag{81}$$

For our measurements, this results in a charge of 2.03×10^{-19} C. Again this confirms the assumption of univalent charges.

V. BEYOND THE MODEL PROBLEM

The theoretical and numerical results presented in this work are all based on a simple and idealized problem: the movement of inert point-charges in a one-dimensional geometry with perfectly blocking electrodes, when a voltage is suddenly applied. We showed that the one-dimensional devices containing a nonpolar liquid with surfactant that we used to obtain the experimental results, are well described by this model problem for a wide variety of parameters. This is, however, an exceptional case: in most practical systems additional effects will play a role, at least for some parameter regions. Also the geometry, the boundary conditions and the initial condition will be less than ideal in most practical applications.

We found approximate analytical solutions in a one-dimensional geometry, but much more complicated dynamics arise in two- or three-dimensional problems. Effects such as tangential conduction in the double layers and recirculating bulk diffusive flow have been shown to arise in even the simplest more-dimensional geometries [31].

Even for one-dimensional problems, the dynamics are much more complicated when the charges are initially not in a homogeneous distribution (for instance, when the polarity of an applied voltage is reversed). In this case, the electric field does not always have to point in the same direction in the whole device. The external electric current has been shown not to decrease monotonically because of this [19].

When charges are forced out of their equilibrium distribution, the (dissociation or disproportionation) reactions that are responsible for their origin will play a role. The continuous generation of new charges prevents the bulk to become completely depleted, and the fluxes of new charges can be in some cases more important than the transient flux of initially existing charges [14].

When the electrodes are not perfectly blocking, a DC current can pass through the cell [32]. Faradaic reactions can result in a diffusion limited current, but also in a reaction limited current leading to space charge at the opposite electrode [33]. Studies which are analogous to the present work, but for nonblocking electrodes, have been carried out [34]. In semiconductors, the Mott-Gurney law for space charge limited current of injected charges is derived on very similar assumptions as the ones made in this work [35].

At large voltages, the concentration of charges near the electrodes can become very high. In these circumstances, charge crowding leads to the necessity to consider steric effects [17,18], correlation effects and solvent interactions. This will be most important in the space charge limited regime, and may in some systems pose a restriction on the formation of space charge layers.

In this work, the liquid in which the charges move is considered to be static. However, in reality the friction force exerted by the medium on the charges (which results in the transport being described by a mobility) leads to a reaction force on the liquid, and electrohydrodynamics have to be included. This results in effects such as induced charge electro-osmosis [36,37] and bulk electroconvection [38,39]. Electrohydrodynamical effects will be most important in more-dimensional geometries, but can even in the one-dimensional problem lead to symmetry-breaking and instability [40].

It is obvious that, for most realistic situations, the Poisson-Nernst-Planck equations have to be extended or even modified to provide a good description. However, the solutions, presented in this work, of the simple model problem in a simple situation provide insights that are useful in more complicated situations.

VI. CONCLUSIONS

We have derived approximate analytical expressions which are solutions of the Poisson-Nernst-Planck equation, and describe charge transport under the influence of an electric field, in four limiting cases. In the geometry limited regime, applicable at low charge contents and high voltages, diffusion, and the effect of the charges on the electric field are neglected. The only restriction on the external current is then the condition that charges cannot move out of the device. This results in a uniform movement of the charges toward the electrodes until the bulk is completely depleted. During this transient, the external current decreases linearly.

In the space charge limited regime, which occurs at high charge contents and high voltages, only diffusion is neglected. Because of the high charge content, we can assume the current density in the device to be homogeneous. This results in transient space charge layers, which screen the field in the bulk almost completely, resulting in a $-3/4$ power law decrease of the current. When the bulk is completely depleted of charges, the space charge layers disappear, the electric field becomes homogeneous again and the current drops quickly to zero.

In the diffusion limited regime, which is valid for low charge contents and low voltages, we neglect the influence of charges on the electric field. Diffusion prevents the charges from separating, which allows us to assume that the total concentration is homogeneous at all times. The resulting external current decreases exponentially.

In the double layer limited regime, applicable at high charge contents and low voltages, the combination of diffu-

sion and screening of the electric field results in thin double layers in which all variations occur. In the bulk all quantities are homogeneous. We solve this regime by assuming that both the current density and the total concentration are homogeneous over the whole device. Charging the double layers results in an exponentially decreasing current.

The analytical results are tested with detailed numerical simulations. The distribution of charges, the electric field and the external current all correspond very well, both in function of time as in function of position. These results provide a better understanding of various nonlinear effects, which are becoming increasingly important in many practical applications in which the Poisson-Nernst-Planck equations are relevant.

The expressions for the external current are also tested against experiments on a mixture of dodecane and a surfactant, providing us a way to determine various important properties of the devices. The good agreement between the results from the different regimes with each other, with numerical fitting and with results from other works are a strong indication of the existence of each of the four regimes.

[1] M. Z. Bazant, K. Thornton, and A. Ajdari, Phys. Rev. E **70**, 021506 (2004).
[2] P. Biler and J. Dolbeault, Ann. Henri Poincare **1**, 461 (2000).
[3] I. Borukhov, D. Andelman, and H. Orland, Electrochim. Acta **46**, 221 (2000).
[4] J. Newman, *Electrochemical Systems* (Prentice-Hall, Englewood Cliffs, NJ, 1991).
[5] I. Rubinstein, *Electrodiffusion of Ions* (SIAM, Philadelphia, 1990).
[6] R. J. Hunter, *Foundations of Colloid Science,* 2nd ed. (Oxford University Press, Oxford, 2000).
[7] J. Lyklema, *Fundamentals of Interface and Colloid Science* (Academic, New York, 1995).
[8] J. W. Jerome, *Analysis of Charge Transport: A Mathematical Study of Semiconductor Devices* (Springer-Verlag, New York, 1995).
[9] J. J. Liou, IEE Proc.-G: Circuits, Devices Syst. **139**, 646 (1992).
[10] P. S. Davids, I. H. Campbell, and D. L. Smith, J. Appl. Phys. **82**, 6319 (1997).
[11] T. Li, P. P. Ruden, I. H. Campbell, and D. L. Smith, J. Appl. Phys. **93**, 4017 (2003).
[12] V. A. Rozhansky and L. D. Tsendin, *Transport Phenomena in Partially Ionized Plasmas* (Taylor & Francis, London, 2001).
[13] D. B. Graves and K. F. Jensen, IEEE Trans. Plasma Sci. **14**, 78 (1986).
[14] F. Strubbe, A. R. M. Verschueren, L. J. M. Schlangen, F. Beunis, and K. Neyts, J. Colloid Interface Sci. **300**, 396 (2006).
[15] M. F. Hsu, E. R. Dufresne, and D. A. Weitz, Langmuir **21**, 4881 (2005).
[16] S. Jayaram and J. D. Cross, J. Electrost. **29**, 55 (1992).
[17] M. S. Kilic, M. Z. Bazant, and A. Ajdari, Phys. Rev. E **75**, 021502 (2007).
[18] M. S. Kilic, M. Z. Bazant, and A. Ajdari, Phys. Rev. E **75**, 021503 (2007).
[19] F. Beunis, F. Strubbe, M. Marescaux, K. Neyts, and A. R. M. Verschueren, Appl. Phys. Lett. **91**, 182911 (2007).
[20] F. Beunis, F. Strubbe, K. Neyts, and A. R. M. Verschueren, Appl. Phys. Lett. **90**, 182103 (2007).
[21] H. De Vleeschouwer, F. Bougrioua, and H. Pauwels, Mol. Cryst. Liq. Cryst. **360**, 29 (2001).
[22] P. Castillo, N. Bennis, M. Geday, X. Quintana, J. M. Oton, F. Beunis, and K. Neyts, Mol. Cryst. Liq. Cryst. **450**, 239 (2006).
[23] B. Comiskey, J. D. Albert, H. Yoshizawa, and J. Jacobson, Nature (London) **394**, 253 (1998).
[24] T. Bert, H. De Smet, F. Beunis, and K. Neyts, Displays **27**, 50 (2006).
[25] I. D. Morrison and S. Ross, *Colloidal Dispersions* (Wiley, New York, 2002).
[26] A. R. M. Verschueren, P. H. L. Notten, L. J. M. Schlangen, F. Strubbe, F. Beunis, and K. Neyts, J. Phys. Chem. A (to be published).
[27] K. Neyts, J. Beeckman, and F. Beunis, Opto-Electron. Rev. **15**, 41 (2007).
[28] V. Novotny, J. Electrochem. Soc. **133**, 1629 (1986).
[29] M. N. Ozisik, *Heat Conduction* (Wiley, New York, 1980).
[30] R. E. Kornbrekke, I. D. Morrison, and T. Oja, Langmuir **8**, 1213 (1992).
[31] K. T. Chu and M. Z. Bazant, Phys. Rev. E **74**, 011501 (2006).
[32] I. Rubinstein and L. Shtilman, J. Chem. Soc., Faraday Trans. **75**, 231 (1979).
[33] A. Bonnefont, F. Argoul, and M. Z. Bazant, J. Electroanal. Chem. **500**, 52 (2001).
[34] K. T. Chu and M. Z. Bazant, SIAM J. Appl. Math. **65**, 1485 (2005).
[35] P. Mark and M. Allen, Annu. Rev. Mater. Sci. **3**, 111 (1973).
[36] M. Z. Bazant and T. M. Squires, Phys. Rev. Lett. **92**, 066101 (2004).
[37] T. M. Squires and M. Z. Bazant, J. Fluid Mech. **509**, 217 (2004).
[38] H. Lin, B. D. Storey, M. H. Oddy, C. H. Chen, and J. G. Santiago, Phys. Fluids **16**, 1922 (2004).
[39] B. D. Storey, B. S. Tilley, H. Lin, and J. G. Santiago, Phys. Fluids **17**, 018103 (2005).
[40] B. Zaltzman and I. Rubinstein, J. Fluid Mech. **579**, 173 (2007).